Eighth Australasian Fluid Mechanics Conference, University of Newcastle, N.S.W., 28 November/2 December 1983.

THE FREE OVERFALL IN A TRAPEZOIDAL CHANNEL

R.J. KELLER AND S.S. FONG

DEPARTMENT OF CIVIL ENGINEERING

MONASH UNIVERSITY, CLAYTON, VIC. 3168 AUSTRALIA

SUMMARY The results of a theoretical and experimental study of the free overfall in a trapezoidal channel are presented. The theoretical analysis involves the application of the momentum equation to a control volume bounded upstream by the critical depth section and downstream by the free overfall section. An appropriate assumption for the pressure distribution at the free overfall is made, based on available measurements in rectangular and triangular channels. Experiments were carried out using a 3m long perspex channel and close agreement between theoretical and experimentally measured end depths is noted. Subsequently a design graph is developed showing the relationship between non-dimensional functions of end depth and discharge. The graph permits the determination of the discharge in a trapezoidal channel from a measurement of the end depth.

NOTATION

A	Cross-sectional area
A_1, A_2	Cross-sectional area components defined in Fig. 2.
B	Water surface width
b	Channel base width
F	Horizontal force
G_1	$X_E + X_E^2$
G_2	$\frac{(3 + 2X_E)X_E}{(1 + X_E)}$
g	Gravitational acceleration
K	$(4/3)k$
k	Pressure factor
k_1, k_2	Pressure factors for triangular and rectangular channels respectively
$k_{equiv.}$	Equivalent pressure factor defined by Eq. (9)
m	Channel side slope
Q	Flow rate
V	Area averaged velocity
X	my/b
y	Flow depth
y_g	Depth to centroid of trapezoidal cross-section
β	Momentum coefficient
γ	Specific weight of water
ρ	Mass density of water

Subscripts

C	Critical section
E	End section (at free overfall).

1 INTRODUCTION

Theoretical and experimental investigations in the past have shown that a relationship exists between the flow rate and the depth at the free overfall of a channel. Such a relationship enables, in principle, the use of the free overfall as a discharge metering structure.

The end depth-discharge relationship for rectangular channels has been extensively studied; for example by Rouse (1936) and Fathy and Shaarawi (1954). Smith (1962) has performed similar studies in circular channels.

Investigations of the free overfall for a trapezoidal channel have been relatively few. The earliest significant study was performed by Diskin (1961) and important published discussions were presented by Rajaratnam et al. (1962) and Replogle (1962). An investigation of the brink depth of a trapezoidal broad-crested weir was presented by Neogy (1972).

In those of the above studies in which the momentum equation was solved to establish a relationship between the end depth and the discharge, a zero pressure distribution at the end section was assumed. However, reports of measurements of the pressure distribution at the end sections by Rouse (1936), Fathy and Shaarawi (1954) and Replogle (1962) indicate that, although small, the end pressure effect is by no means negligible. Rajaratnam et al. (1962) and Neogy (1972) developed a relationship linking the critical and end depths taking into account the pressure at the end section. However, in neither case were the resulting equations solved because of the complexity of their terms.

In this paper the results of an experimental and theoretical study of the free overfall in a trapezoidal channel are presented. In the theoretical analysis the pressure distribution at the end section is included in a momentum analysis and the resulting equations are successfully solved.

Herein the theoretical analysis and method of solution are reviewed briefly. The experimental facilities and techniques are then described and the results compared with the predictions of the theoretical model. A calibration chart is then presented from which for any shaped trapezoidal channel, the discharge can be predicted for a given end depth. Conclusions and recommendations for further work complete the paper.

2 THEORETICAL STUDY

2.1 Physical Description

As flow approaches a free overfall, the mean velocity increases considerably and strong vertical curvature of the flow profile is evident. There is a consequent strong departure from hydrostatic pressure distribution along the approach to the overfall and at the end section the pressure at the upper and lower nappe of the flow is atmospheric. Within the flow at the end section the pressure is non-atmospheric.

At distances well upstream of the overfall, vertical accelerations are negligible and a hydrostatic pressure distribution can be safely assumed. A section occurs where the depth is critical and this forms the upstream boundary of the control volume for the momentum equation analysis.

2.2 Assumptions

The following assumptions are made in applying the momentum equation:

(a) The channel slope is hydraulically mild and sufficiently small that the weight component of the water within the control volume resolved down the slope can be neglected.

(b) The pressure distribution at the section of critical depth (the upstream boundary of the control volume) is hydrostatic.

(c) The pressure distribution at the end depth section is a quadratic parabola with a peak pressure head of ky where k is the pressure factor and y the depth. This assumption follows from measurements of the pressure distribution at the overfall of non-trapezoidal channels by Fathy and Shaarawi (1954) and Replogle (1962). In fact these measurements showed a slightly skewed parabolic shape for the pressure distribution. However, Fong (1982) has shown that the error involved in assuming a quadratic parabolic shape is negligible. Discussion of the magnitude of the pressure factor k is deferred until Section 2.4.

(d) The momentum coefficient, β, has the value of unity. The validity of this assumption has been demonstrated by Replogle (1962).

(e) Shear forces arising from contact of the moving water with the channel boundaries are negligible. This assumption follows from the short length of the control volume and the large differential between the pressure forces at the upstream and downstream ends of the control volume.

2.3 Theoretical Analysis

With reference to Figure 1, application of the momentum equation to the control volume yields

$$Q\rho V_E - Q\rho V_C = F_C - F_E \qquad (1)$$

where Q is discharge, ρ is fluid density, V is velocity, F is horizontal force, and subscripts E and C refer respectively to the end section and the critical section.

Fong (1982) has shown that the horizontal force terms are given by

$$F_C = \gamma A_C \, y_{gC} \qquad (2)$$

$$F_E = \frac{4}{3} \, kA_E \, y_{gE} \qquad (3)$$

where γ is the fluid specific weight, A is cross-sectional area and y_g is the distance from the surface to the centroid of the cross-section. Noting further that V = Q/A and that

$$Q^2 = \frac{g \, A_C^3}{B_C} \qquad (4)$$

where B is the surface width, Eq. (1) may be rearranged to the form

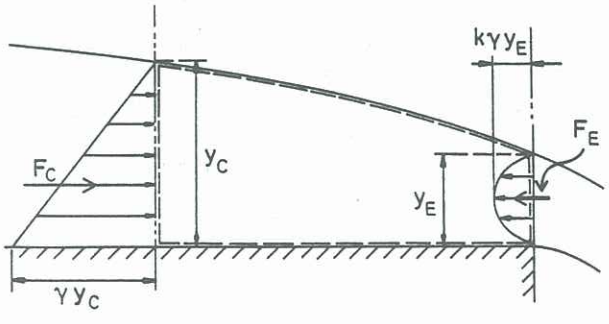

Figure 1 Control Volume for Theoretical Analysis.

$$\frac{A_C}{B_C}\left(\frac{A_C^2}{A_E} - A_C\right) = A_C \, y_{gC} - K \, A_E \, y_{gE} \qquad (5)$$

where K = 4/3 k.

Fong (1982) has shown further that

$$y_{gC} = \frac{3 + 2X_C}{6(1 + X_C)} \, y_C \qquad (6a)$$

$$y_{gE} = \frac{3 + 2X_E}{6(1 + X_E)} \, y_E \qquad (6b)$$

$$\frac{A_C}{B_C} = \frac{(1 + X_C)}{(1 + 2X_C)} \, y_C \qquad (7)$$

where X = my/b, m is the side slope (m horizontal to 1 vertical), and b the base width.

Substitution of Eqs. (6) to (7) in Eq. (5) and rearrangement yields

$$10X_C^4 + 20X_C^3 + 9X_C^2 - \frac{6}{G_1}(X_C^3 + 3X_C^4 + 3X_C^5 + X_C^6) - K \, G_1 \, G_2 \, (1 + 2X_C) = 0 \qquad (8)$$

where $G_1 = X_e + X_E^2$

$$G_2 = \frac{(3 + 2X_E) \, X_E}{(1 + X_E)} \, .$$

Equation (8) links the depth at the end section y_E to the critical depth y_C, and hence through Eq. (4), to the discharge, Q. The form of Eq. (8) is complicated and the terms appear to the sixth power. Solution difficulties have in fact been the main reason for the assumption of zero pressure at the end section in previous studies.

In the present study Eq. (8) was solved iteratively using the Newton Raphson method. For a given value of y_E, a value of y_C can be guessed and successively more accurate values obtained by iteration. Full details of the procedure are contained in Fong (1982). Computations were performed on the Monash University VAX computing system.

2.4 End Section Pressure Distribution Factor.

Solution of Eq. (8) requires an estimate of the pressure distribution factor, k. Measured values in trapezoidal channels have not yet been obtained, so in the present study an equivalent value was deduced from measurements by Replogle (1962) in a 90° triangular channel and in a rectangular channel. With reference to Figure 2 an area weighted value of k was determined from

$$k_{equiv} = k_1 \frac{A_1}{A_1 + A_2} + k_2 \frac{A_2}{A_1 + A_2} \qquad (9)$$

Replogle (1962) has presented values for k of 0.175 for a triangular cross-section and 0.215 for a rectangular cross-section. Substitution of these values into Eq. (9) and use of the equality $X_E = my_E/b$ yields [Fong (1982)]

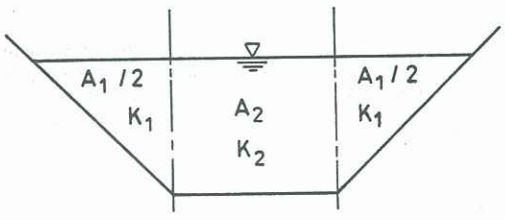

Figure 2 Definition Sketch for Equivalent Pressure Factor

$$K = \frac{4}{3} k_{equiv.} = \frac{4}{3} \frac{(0.215 + 0.175\ X_E)}{(1 + X_E)} \qquad (10)$$

Equation (10) was utilized for the factor K in Equation (8).

3 EXPERIMENTAL STUDY

Suitable dimensions were determined for a flume to obtain experimental data to verify the theoretical model. The side slope selected was 1:1 and the base width, 0.150m. These dimensions were adopted to suit the maximum available water supply of 20 litres/sec., thereby ensuring a sufficiently large end depth for accurate measurements. The length of the flume was 3m, chosen to be in excess of twenty times the critical depth associated with the largest test discharge. A bed slope of 1:1500 was adopted to ensure sub-critical flow at all test discharges.

The channel was fabricated from 6mm perspex sheet supported by a steel frame. The flow entered the channel via an inlet tank which considerably decreased the turbulence of the incoming water. The flow rate was monitored by a magnetic flowmeter on the supply pipe, ensuring an accuracy in discharge measurement of ± 0.5%.

Measurements of the end depth and of the longitudinal water surface profile upstream from the brink were made with a Vernier pointer gauge mounted on a trolley. The trolley ran on precisely levelled rails, supported in turn by the steel frame. Adequate sizes were selected for all supporting members to ensure rigidity and minimal deflection.

Figure 3 shows a schematic of the test set-up.

Measurements of the flow rate and the corresponding end depths were performed for 47 flows ranging from 6.13 to 23.19 l/sec. End depths were measured with the pointer of the Vernier just touching the water surface. Minor fluctuations caused by surface disturbances arising from cross waves were observed during some tests. However, time and care taken during the measurements ensured that their accuracy was not seriously compromised by this phenomenon. For selected flows, longitudinal flow profiles were measured.

4 RESULTS AND DISCUSSION

For the experimental flume of given side slope and base width, a theoretical curve linking discharge and end depth was developed using Eq. (8) and the solution procedures described briefly in Section 2. This theoretical curve is shown as a solid line in Fig.4. Superimposed on Fig. 4 are the experimental data obtained in the present study.

Also superimposed on Fig. 4 is a dashed line representing a theoretical relationship between end depth and discharge with the assumption of zero pressure throughout the fluid at the end section.

The figure shows very good agreement between the experimental data and the theoretical relationship developed herein. Almost all of the experimentally measured end depths were within ± 3% of the predicted values. It is clear that a calculated end depth-discharge relationship for which the pressure distribution at the overfall is not included under-predicts the end depth by up to 7% or, of more relevance to the hydraulic engineer, over-predicts the discharge for a given end depth by up to 11%.

The very good agreement evident in Fig. 4 could be made even better by "fine-tuning" the relationship for pressure factor, Eq. (9). However in the absence of specific measurements of the pressure distribution at the end section of a trapezoidal channel, such an adjustment is unwarranted.

For twenty-one of the tests the water surface profile upstream from the end section was measured. From these profiles the position at which the flow was critical was noted.

A plot of flow rate against distance from the brink to the critical section showed a trend of increasing distance with flow rate although the scatter of the data points was high. Further, this distance normalised with the critical depth was plotted against the non-dimensional discharge. Again, however, significant data scatter was evident and no correlation could be obtained.

These plots have been presented by Fong (1982) but are not reproduced here because of their inconclusive nature. Diskin (1961) reported that the critical depth occurred between 2 y_c and 3 y_c upstream from the end section. The data from the current study indicate a distance of between 2.4 y_c and 3.6 y_c.

5 CALIBRATION CHART

Following the very good agreement between the theory and the experimental data from the present study, a calibration chart is formulated from which the discharge in any given trapezoidal channel can be obtained from a measurement of the end depth. From the theoretical equation [Eq. (8)] values of the

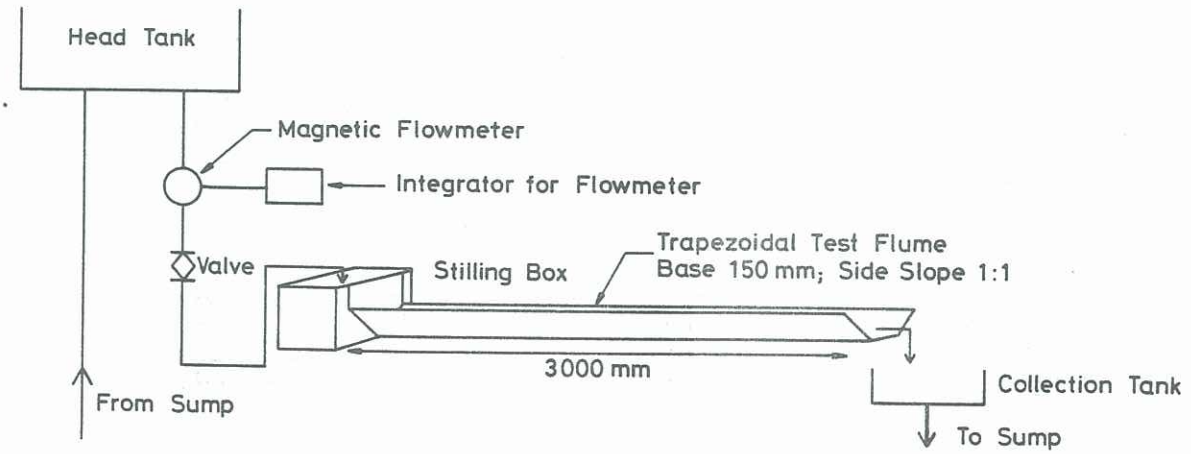

Figure 3 Schematic of Experimental Test Rig.

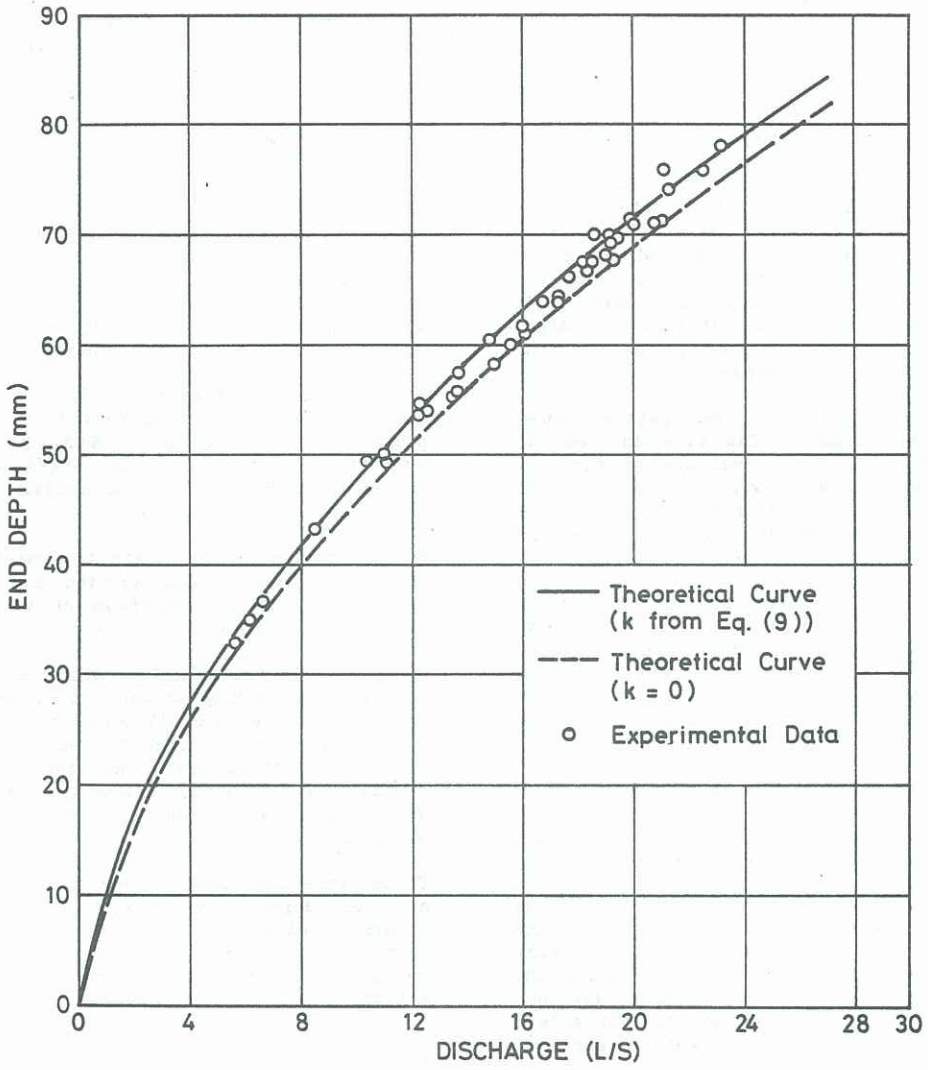

Figure 4 Comparison between Theory and Experimental Data.

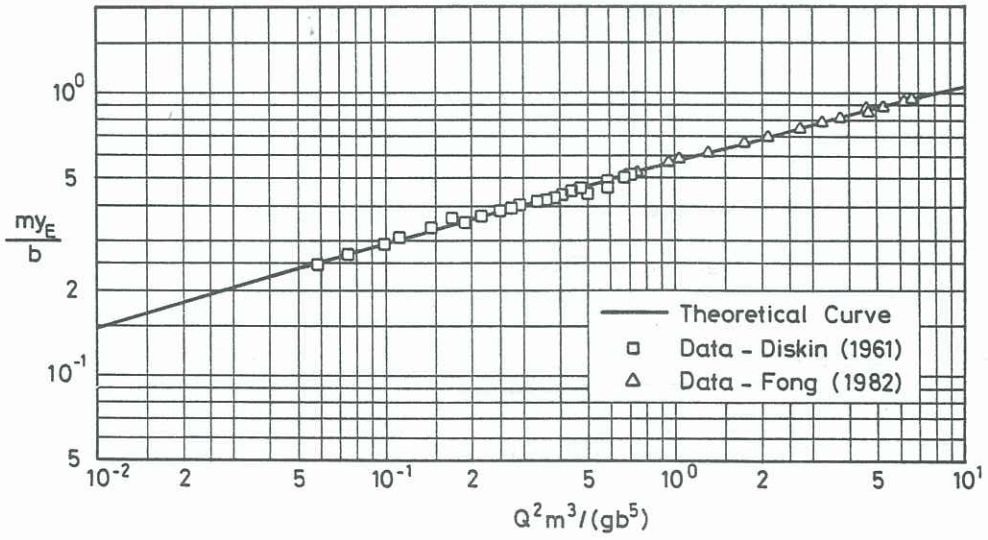

Figure 5 Calibration Chart for Trapezoidal Free Overfall.

non-dimensional parameters $\frac{m\, y_E}{b}$ and $\frac{Q^2\, m^3}{g\, b^5}$ were generated and plotted. The plot, presented in Fig. 5, allows the determination of the discharge from a measured value of y_E and known values of m and b.

Superimposed on the plot are the data from both the present study and from the study of Diskin (1961). The figure indicates again the excellent nature of the agreement between the theory presented herein and the available data.

Despite this excellent agreement it is recommended that the chart be used with caution because of the limited nature of the available data. Further corroboration with channels of different bed width and side slope is recommended.

6 CONCLUSIONS AND RECOMMENDATIONS

On the basis of the theoretical and experimental studies reported herein, the following conclusions are drawn and recommendations made:

(i) The assumption of a parabolic pressure distribution at the free overfall results in a better estimate of the end depth-discharge relationship than a solution which assumes zero pressure. The theoretical solution presented herein predicts the experimental data to within the assessed experimental error.

(ii) The longitudinal water surface profile data indicate that the critical depth section occurs at distances between 2.4 y_c and 3.6 y_c upstream of the free overfall. However, the data are scattered and it remains unclear whether or not a relationship exists between the flow-rate and the position of the critical depth.

(iii) A theoretically derived non-dimensional calibration chart shows excellent agreement with the available data. It permits in principle the determination of the discharge in a trapezoidal channel of given base width and side slope from a measurement of the end depth. However, it is emphasised that the available data is limited and that further corroboration of the calibration chart should be obtained.

(iv) To the authors' knowledge no measurements of pressure distribution at the end section of a trapezoidal channel have been performed. In the study reported herein a parabolic pressure distribution has been utilized whose shape was deduced from available measurements in rectangular and triangular channels. Future studies should include the measurement of pressure distribution at the end section of different trapezoidal channels to enable further refinement of the model presented herein.

7 REFERENCES

DISKIN, M.H. (1961) End Depth at a Drop in Trapezoidal Channels. J. Hyd. Div., Proc. ASCE, 87, HY4, pp. 11-32.

FATHY, A and SHAARAWI, A.M. (1954) Hydraulics of the Free Overfall. Proc. ASCE, 80, Separate No. 564, December.

FONG, S.S. (1982) Experimental and Theoretical Study of the Free Overfall in a Trapezoidal Channel, M.Eng.Sc. Thesis, Monash University.

NEOGY, B.N. (1972) Brink Depth for Trapezoidal Broad-Crested Weir. J. Hyd. Div., Proc. ASCE, 98, HY12, pp. 2171-2189.

RAJARATNAM, N., SUBIR KAR and HAMID, H.I. (1962) Discussion of Diskin (1961). J. Hyd. Div., Proc. ASCE, 88, HY1, pp. 119-136.

REPLOGLE, J.A. (1962) Discussion of Diskin (1961). J. Hyd. Div., Proc., ASCE, 88, HY2, pp. 161-165.

ROUSE, H. (1936) Discharge Characteristics of the Free Overfall. Civil Engineering, ASCE, 6, No. 4, pp. 257-260.

SMITH, C.D. (1962) Brink Depth for Circular Channels, J. Hyd. Div., Prov. ASCE, 88, HY6, pp. 125-134.